Macromolecular Materials and Engineering
Open Access
www.mame-journal.de

Recent Developments in Additive Manufacturing of Conductive Polymer Composites

*Tomasz Blachowicz, Guido Ehrmann, and Andrea Ehrmann**

Additive manufacturing, also named 3D printing, can be used to create objects from diverse polymers, metals, and other materials in diverse shapes and dimensions. If special physical or chemical properties are necessitated, using corresponding feedstock enables varying such properties in a broad range. Besides choosing a suitable base material, often composite materials are used for specific applications. Here, an overview of recent developments in 3D printing of polymer composites with conductive properties is given. After a definition of conductivity ranges and the respective potential applications, additive manufacturing methods applicable for these polymer composites as well as potential resistivity or resistance measurement methods are reported. An overview of the most recent reports of 3D printing polymer composites with different conductive fillers is followed by a summary of the applications found in the recent literature.

1. Introduction

While additive manufacturing techniques are mostly used for rapid prototyping or rapid manufacturing of objects having specific shapes or fulfilling defined mechanical requirements, nowadays 3D printing methods are extended towards materials with specific physical or chemical properties. 3D printed parts can be used in optics[1] or microfluidics,[2] can have magnetic[3] or conductive[4] and many other properties. While some of these properties can be achieved by adding a small amount of suitable micro- or nanoparticles to the 3D printing polymer, conductivity is distinctive since here a certain minimum of conductive material is necessary to form percolation paths inside the material.[5,6] Below this percolation threshold, such a composite material show no conductivity, and even higher concentrations of the conductive filler are necessary to reach conductivities enabling using the material as parts of conductive circuits.[7,8] This, on the other hand, may destabilize the composite structure in comparison to the pure polymer.[9] Additive manufacturing of conductive composites, on the other hand, has many potential applications, such as sensors and actuators, biomedicine and biotechnology, electromagnetic interference shielding, etc. While some of these applications can also use conventional techniques such as injection molding, 3D printing offers a much higher degree of freedom regarding the shape of the produced objects as well as the possibility to produce single objects at lows costs, without the necessity to prepare a cost-intensive mold or other tools.

This optimization problem, combined with an increasing need to prepare 3D printed objects from conductive materials for diverse applications, has led to an increase in the research carried out on 3D printable conductive polymer composites, as **Figure 1** shows. The increasing amount of research in this field suggests reviewing the recent state of research and technology. The aim of this review paper is to support researchers interested in conductive 3D printed composite which either come from the material side and want to develop materials and 3D printing further, or which come from the application side and are interested in the possibilities to use additive manufacturing instead of other techniques. It thus contains not only information about the most recent research results in this area, concentrating on the scientific literature of the last five years, but also technical information about definitions and measures of conductivity, 3D printing techniques, and intrinsically conductive polymers, before potential applications are reported.

The paper is structured as follows: Starting with an overview of conductivity ranges and techniques to measure conductive or resistance, respectively, we briefly introduce different polymer-based additive manufacturing techniques which are mostly used to print conductive polymer composites. 3D printing with conductive polymers is reviewed for fused deposition modeling (FDM), stereolithography (SLA), powder-bed methods, and other techniques, before an overview is given of potential applications of such 3D printed conductive objects, depending on their conductivity.

T. Blachowicz
Institute of Physics—Center for Science and Education
Silesian University of Technology
Gliwice 44-100, Poland

G. Ehrmann
Virtual Institute of Applied Research on Advanced Materials (VIARAM)
33619 Bielefeld, Germany

A. Ehrmann
Faculty of Engineering and Mathematics
Bielefeld University of Applied Sciences
Interaktion 1, 33619 Bielefeld, Germany
E-mail: andrea.ehrmann@fh-bielefeld.de

The ORCID identification number(s) for the author(s) of this article can be found under https://doi.org/10.1002/mame.202200692

DOI: 10.1002/mame.202200692

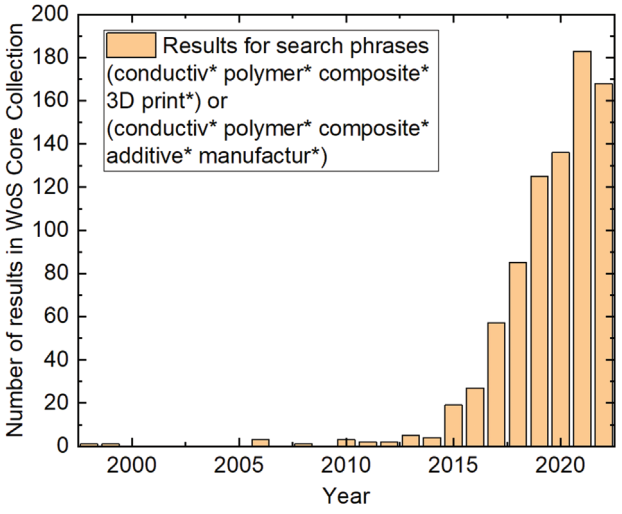

Figure 1. Numbers of results in the Web of Science Core Collection for the search phrases (conductive* polymer* composite* 3D print*) or (conductive* polymer* composite* additive* manufactur*), measured November 27, 2022.

2. Conductivity

Before discussing conductive polymer composites and their potential applications, it is necessary to define conductivity ranges and the methods to measure conductivities of one-dimensional structures (lines), two-dimensional structures (surfaces) and three-dimensional objects (bulk materials). Besides, the differences between physical properties related to conductive materials as well as corresponding units are given, including a pseudo-unit often found in scientific literature, which is not in accordance with the SI standard. We believe that excluding sources of error in measurement and in communicating the gained data belongs to the scopes of a helpful review papers, thus these points are discussed here, although measurement methods are very often not mentioned in the papers discussed below.

2.1. Definitions of Conductivity and Similar Parameters

The electrical resistivity ρ is a material parameter, correlated with the electrical conductivity σ by $\sigma = 1/\rho$. The unit of ρ is Ω m (Ohm × meter), while the unit of the conductivity is $1/(\Omega\ \mathrm{m}) = \mathrm{S\ m^{-1}}$ (Siemens per meter).

Assuming a conductive wire or a similar long object with a length l and a cross-section A, its resistance R is defined as $R = \rho l/A$. The conductance is the inverse of the resistance. The unit of the resistance is Ω, while the conductance has the unit S (Siemens).

Besides these direct current values, it is also possible to use alternating current measurements with different frequencies, resulting in the electric impedance $Z = R + iX$ with the real part R (resistance) and the imaginary part X (reactance).[10] Impedance measurements can, e.g., measure the water content of a human body part.[11,12] The impedance has the same unit as the resistance, i.e., Ω.

2.2. Measurement Methods for Conductive Objects

Resistance measurements are most often performed with the so-called two-point technique, meaning that a resistance-meter, often in the form of a multimeter, has two tips contacting the object to be investigated.

In any resistance measurement, however, a contact resistance will occur. If this contact resistance is not significantly smaller than the resistance which should be measured, the contact resistance will cause a systematic deviation between measured and real values. This problem can be overcome by using a four-point technique in which a well-defined current is applied between two outer contact points with a wire or bar, while two additional inner contact points are used to measure the voltage between them.[13] In this way, the contact resistance can approximately be excluded from the measured value.

An often measured value is the sheet resistance of a foil, a coating or other thin samples with relatively large lateral dimensions, generally much larger than the measurement area. For such measurements, commercial four-point instruments with four equidistant in-line contacts can be used which are pressed on the sample. The sheet resistance is then calculated as $R_s = 4.532\ V/I$, automatically given by commercial instruments.[14] It should be mentioned that the unit of the sheet resistance is simply Ω. Any additions, such as "$\Omega\ \mathrm{sq^{-1}}$" or "$\Omega/\square$", do not have any physical meaning and should thus not be misused to indicate that a sheet resistance is meant.

If sheet resistance measurements on surfaces with complicated shapes are necessary, or if the surface of a sample should not be touched by electrodes, the so-called van der Pauw technique can be used, in which four contacts are attached to the sample edges, and by varying the contacts for current and voltage, a mathematical formula can be applied to these results to gain a sheet resistance.[15]

Besides the aforementioned potential problem of large contact resistances or measuring small resistance values, respectively, the opposite problem of very large resistances must also be taken into account. In this case, large voltages are necessary to reach a certain measurable current through the material under investigation, which would be dangerous in case of using a common multimeter. Instead, commercially available teraohm meters can be used to measure sheet resistance as well as the resistance from top to bottom through a thin layer.[16]

Regarding 3D printed conductive polymer composites, one additional factor should be taken into account, which may cause problems in all aforementioned measurement techniques, i.e., the surface roughness. Many commercial electrodes are not intended to be used on uneven or soft surfaces. In these cases, a well-known method is given by applying silver-paint onto the surface to produce a proper contact. Generally, it is always necessary to ensure a proper, reliable contact to the surface. Besides, standard procedures of measurement technology have to be taken into account, such as performing a sufficient number of nominally identical measurements and giving standard deviations in addition to averages, testing and calibrating the measurement equipment before use, checking the measurement setup carefully, etc.

Besides these direct measurement techniques, there are several contactless techniques which can be used in case contacting

measurements are not suitable for a special situation.[17] These techniques, however, will not be described here in detail as they are scarcely used for investigations of conductive polymer composites.

2.3. Ranges of Conductivity

As mentioned in the previous section, a broad range of resistivities can be expected in such measurements, typically between the order of 10^{-8} Ωm and 10^{18} Ωm, depending on the material under investigation.[13] Polymers are mostly insulators, with typical resistivity higher than 10^{4} Ωm, while metals are usually conductors, with a typical resistivity below 10^{-5} Ωm.[18] The intermediate resistivity region contains semiconductors which are not in the scope of this review.

It must be mentioned, however, that "conductive" in discussions of 3D printed polymer composites does not necessarily mean "metallic conductance", but can also describe materials with much larger resistivity. This means that evaluating the literature about conductive 3D printed polymer composites necessitates distinguishing between conductivity or resistivity, respectively, in a broad range of more or less conductive materials which can, correspondingly, be used for quite different applications, from printed circuits to heating to electromagnetic interference (EMI) shielding.

3. Polymer-Based 3D Printing Techniques

This section briefly introduces the techniques most often used for polymer-based 3D printing; more detailed descriptions of more additive manufacturing technologies can be found, e.g., in Refs.[1–3]

One of the most often used 3D printing techniques is FDM printing. Besides high-quality FDM printers, a broad variety of low-cost models from diverse companies exist, normally easy to use and relatively small, making FDM printing also interesting for private use, schools, small companies etc. Before printing, a slicer software is used to cut the CAD model into layers of defined height and to define optimum paths, based on parameters adjustable by the user, such as nozzle and printing bed temperatures, printing speed, infill pattern, infill percentage, layer height, etc.[19] In the FDM process, thermoplastic filaments are extruded through a hot nozzle, so that the softened material can be placed along these paths on a printing bed or on a previously printed layer, respectively.[20] Among the most often used FDM printing materials, there are polylactic acid (PLA), acrylonitrile butadiene styrene (ABS), nylon (polyamide), thermoplastic polyurethane (TPU), and several others, all with different mechanical properties and different requirements regarding the printing process, mostly with relatively low melting points to enable easier printing.[21,22] Besides the relatively low mechanical properties of most consumer-grade FDM polymers, dimensional accuracy upon shrinking after the polymer cooled down, warping of especially long, flat objects due to uneven shrinkage in unheated building environments and large waviness based on the filament placement process are typical problems of FDM printed objects, making it often challenging to prepare objects with the required mechanical and morphological properties.[23–25]

While FDM feedstock are polymer filaments, stereolithography (SLA) is based on the photopolymerization of fluid photosensitive resins.[26] Other methods working with photosensitive resins are digital light processing (DLP), liquid crystal display (LCD), multijet printing (MJP), two-photon polymerization (2TPP), continuous liquid interface production (CLIP), etc., using different strategies to illuminate the liquid resin at defined positions.[27] Although these photopolymerization methods can usually create much finer structures than FDM, especially in case of 2TPP, they nevertheless may have problems with dimensional accuracy[28,29] and aging.[30,31]

Powder-bed methods can work with polymers, metals, or even polymer/metal hybrid objects.[32] Besides the well-known selective laser sintering (SLS), other techniques such as high-speed sintering (HSS) or multijet fusion (MJF) can be used to prepare polymer objects.[33] Besides these methods based on locally heating the upper powder layer over the material's melting point, binder jetting applies liquid binder on the powder surface.[34] Powder-bed methods have the advantage that no support structures are needed for protruding parts and a large range of materials is available for them.[35] Nevertheless, these methods may also be challenging in terms of powder size and distribution,[36] dimensional accuracy,[37] and necessitate post-processing.[38,39]

Other methods which are often used are direct ink writing (DIW) based on a inks with well-defined viscosity,[40,41] 3D printing of hydrogels based on thixotropic (shear-thinning) polymer inks,[42,43] and other techniques, used for diverse applications and polymeric materials.

Amongst the here mentioned 3D printing methods, FDM and SLA are generally most often used for polymers. For both techniques, inexpensive printers are available. FDM hast the additional advantage that the filaments are often nontoxic, while SLA resins are, in the form of monomers, usually toxic and thus not well suited for use at home or in schools.

3D printing intrinsically conductive polymers and polymers with conductive fillers is also most often reported for FDM printing, followed by SLA and powder-bed methods. Each of these methods has their own advantages and disadvantages: FDM necessitates preparation of a suitable conductive filament and thus a high-quality filament extruder; if this equipment is available, the actual FDM printing process is similar for many materials and thus less error-prone than, e.g., powder-bed methods which necessitate intensive investigations to optimize the process parameters. Besides, a few conductive filaments are commercially available and thus offer the easiest start to 3D printing of conductive objects. SLA allows adding conductive nanoparticles to the resin without applying an additional instrument; however, as some researchers report in the literature, agglomeration, and sinking of the nanoparticles are issues which have to be taken into account, making the printing process much more challenging. Powder-based methods, finally, enable mixing conductive and nonconductive materials and usually show less agglomeration of the conductive parts, while the aforementioned process parameters are crucial to optimize, and printing mixed materials from a powder-bed can in the worst case become impossible for strongly differing melting temperatures or other physical properties. As the literature shows, each research group thus prefers other techniques, depending on the available equipment and the

planned application, defining the required material and shape parameters of the 3D printed objects.

4. 3D Printing Conductive Polymer Composites

This chapter reviews the most recent literature found in Google Scholar for the search phrase "3D printing conductive polymer" for a time span starting in 2018. Google Scholar was chosen to avoid ignoring the latest conference papers which are usually indexed in the Web of Science with a severe delay. The chapter is subdivided into different ways to produce conductive printable polymers. Additional potential applications are given in Section 5.

4.1. Intrinsically Conductive Polymers

Well-known conductive polymers are polyaniline (PAni), polypyrrole (PPy), poly(3,4-ethylenedioxythiophene):polystyrenesulfonic acid (PEDOT:PSS), pure PEDOT, or polythiophene (PTh), which can be used to produce light-weight, flexible conductive paths or electronic devices.[44] Their adjustable electronic conductivity is based on a π-conjugated orbital structure enabling electron transport.[45] Such conductive polymers are often available in the form of low-viscous solutions, but can also be blended with polymers or other thickeners to fit the viscosity to the requirements of a certain 3D printing technique.[46,47] While many 3D printing approaches for conductive polymers use conductive inks, another broad area of research and development are conductive polymer hydrogels from the aforementioned conductive polymers.[48] Such conductive hydrogels can be influenced by environmental conditions and thus be used as sensors or actuators in different areas of application.[49,50] They are often printed by inkjet or screen printing techniques.[51]

4.2. 3D Printing Intrinsically Conductive Polymers

PEDOT:PSS belongs to the most often used conductive polymers for 3D printing. Yuk et al. prepared a conductive polymer ink based on PEDOT:PSS for 3D printing soft microstructures.[52] To prepare a paste-like conductive ink, they used cryogenic freezing of an aqueous PEDOT:PSS solution, which was afterward lyophilized and dispersed again in a mixture of water and dimethyl sulfoxide (DMSO). They found this ink to be printable with a resolution of ≈30 µm and a high aspect ratio of more than 20 layers printed on top of each other. The printed objects were dry-annealed to reach pure PEDOT:PSS structures with a high electrical conductivity of more than 1.5×10^4 S m^{-1}. By allowing these micro-structured 3D printed objects to swell in a wet environment, they became soft hydrogels with reduced, but still good conductivity ≈2.0×10^3–3.0×10^3 S m^{-1}. A similar approach was chosen by Rastin et al. who prepared a conductive bioink in which they combined PEDOT:PSS with methylcellulose and kappa-carrageenan, resulting in highly thixotropic behavior with its viscosity tunable by varying the polymer concentrations.[53] This ink was found to be in vitro biocompatible and thus useful especially for biomedical applications of conductive objects.

PEDOT: PSS-based hydrogels were prepared, e.g., by Heo et al. who used crystallized PEDOT:PSS for this task.[54] Firstly, the commercially available PEDOT:PSS was deep-frozen at −80 °C for 1 day and afterward lyophilized for 3 days. The resulting PEDOT:PSS solid was then dissolved again in distilled water with ethylene glycol, to which polyethylene glycol diacrylate (PEGDA) with a photo-initiator was added to make the solution photocurable. This solution could be poured on a glass slide or 3D printed in a modified FDM printer, photocuring defined positions by a solid-state UV laser, coupled into a fiber optic, while the solution is placed in a petri dish on top of which a microscope slide works as the printing bed.[55] The whole process is depicted in **Figure 2**.[54]

The so-produced samples were investigated with respect to their mechanical, electrical, and biocompatible properties.[54] The authors found that the PEDOT:PSS content reduced the crosslinking efficiency due to a decrease in transparency, while the compressive stiffness was still higher than for pure PEDOT:PSS hydrogels due to the addition of PEDGA. Sheet resistances were found between ≈0.7 kΩ and 2.7 kΩ. Regarding proliferation and viability of dorsal root ganglion (DRG) cells, a significant increase of both values with increasing PEDOT:PSS content was found which the authors attributed to combining crystallized PEDOT:PSS with poly(ethylene glycol) (PEG) in a hydrogel instead of using pure nonconductive PEG as a hydrogel. The authors thus suggested using the developed hydrogel blend as a potential neural differentiation culture system, but also for other bioelectrical applications.[54]

Wei et al. described a different approach to prepare 3D printed hydrogel structures containing PEDOT:PSS and poly(vinyl alcohol) (PVA), partly with added phenol, supported by Ru(II) as a catalyzer.[56] 3D printing was performed using a syringe with 390 µm nozzle on a robot arm after adjusting the conductive precursor's viscosity by adding hydroxyethylcellulose (Q10); the sol-gel transition of the printed material was triggered by visible light irradiation and finished after ≈30 s for samples without phenol. The authors reported a temperature-dependent conductivity of max. 3.5 S m^{-1} at a temperature of 80 °C and around 1 S m^{-1} at 0 °C. On the other hand, the resistance of different 3D printed shapes depended strongly on the strain, with ≈100% deviation from the value of the unstrained object at a maximum strain ≈40%. They suggested using the developed material as a 3D-printed capacitive force sensor or a temperature-responsive device.

While both aforementioned studies used different procedures similar to SLA based on FDM printers, a customized SLA printer was applied by Scordo et al. to produce conductive polymer cubes of defined dimensions.[57] The authors combined PEGDA with the crosslinking agent Irgacure 819 and filled this resin with different amounts of PEDOT particles to produce dry samples, i.e., no hydrogels as described before. They reported a conductivity of ≈5 S m^{-1} for a PEGDA:PEDOT ratio of 5:1 which was the optimum balance regarding printability and conductivity.

Another approach was chosen by Zhang et al.[58] and Tomaskovic–Crook et al.[59] who used direct-write printing of PEDOT:PSS pillars with high aspect ratio in an array. They applied a self-built scanning ion conductance microscope with a micropipette through which the extruded material is placed on a slowly lowered building plate. The printing process and the

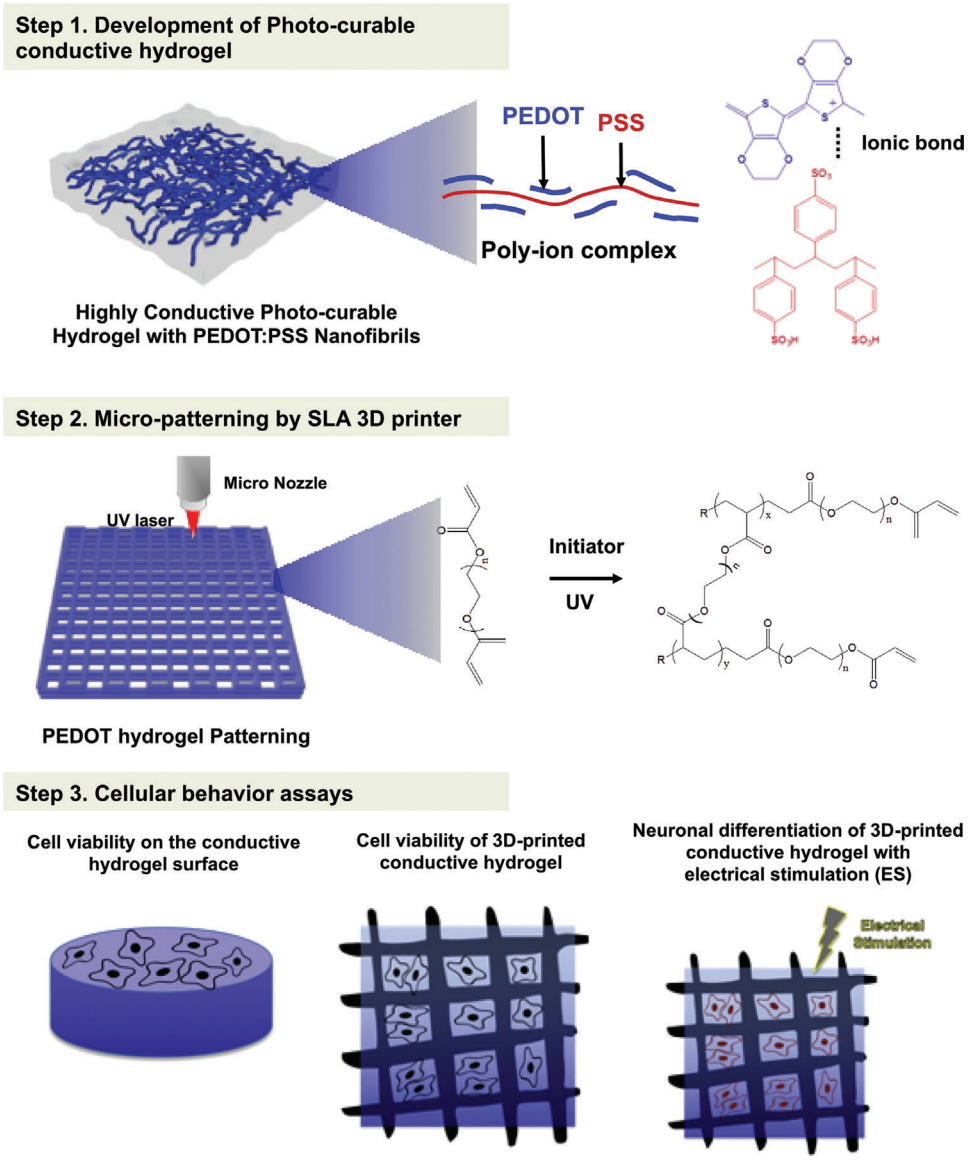

Figure 2. Schematic of the process to fabricate 3D conductive structure using SLA printing system and cellular behavior assays. Reproduced with permission.[54] Copyright 2019, Elsevier.

results are depicted in **Figure 3**.[59] Impedance measurements showed a resistance ≈30 kΩ for a frequency of 100 Hz which increased with time and neuro-cytocompatibility of this tissue engineering platform.

Besides these studies based on PEDOT:PSS, 3D-printed parts from PPy and PAni can also be found in the recent literature. Cullen and Price prepared a photosensitive PPy resin for micro-SLA to enable 3D printing of microscale structures.[60] Due to the problem that PPy photocurable resins tend to producing brittle structures, the authors added extended urethane dimethylacrylate (UDMA) to improve the blended polymer's mechanical properties from the brittle behavior of pure PPy towards a more flexible polymer. The formulation's viscosity was reduced by diluting the UDMA with propylene carbonate. The photoinitiator consisted of silver nitrate, enabling photopolymerization of pyrrole and UDMA. Printing was performed using DLP, reaching feature resolutions ≈30–150 µm, depending on the exposure energy. The authors reported conductivities 10^{-6}–1.0 S m^{-1} for UDMA contents of 75%–15%.

Vijayavenkataraman et al. printed patterns with linewidths ≈30–44 µm from PPy/poly(caprolactone) (PCL) blends by electrohydrodynamic jet (EHD) printing.[61] This technique uses a high voltage to control the EHD jet in the near-field around the nozzle.[62] The PCL/PPy scaffolds showed conductivities ≈0.03–0.12 S m^{-1} and improved growth and differentiation of peripheral neuronal cells in vitro.[61] The authors thus suggested using these scaffolds for guidance conduits in nerve tissue regeneration.

Wibowo et al. used PAni instead to prepare electroactive scaffolds.[63] PAni contents below 1% in screw-assisted extrusion 3D printed scaffolds were found cytocompatible, as tested via

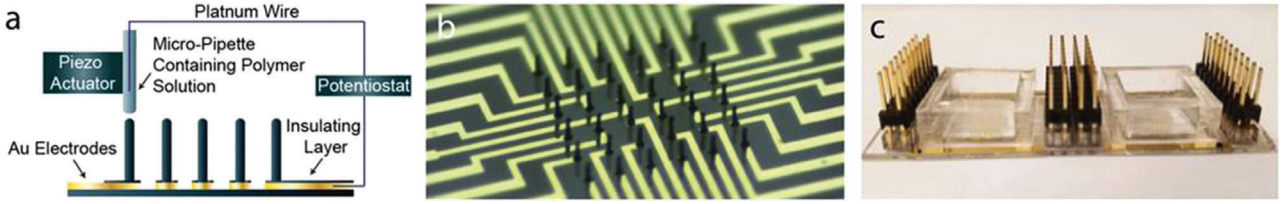

Figure 3. Assembly and use of integrated 3D electrical stimulation tissue engineering platform, including printed conductive polymer pillars in an array. a) Direct write printing of 3D CP pillars by scanning ion conductance microscope. b) Printed individually addressable 3D pillar (height: (80 ± 2) µm and diameter (14 ± 1) µm) electrodes. c) Assembled 3D microelectrode array with connection pins and conductive polymer pillar electrodes within bonded poly(dimethyl siloxane) wells. Reproduced with permission.[59] Copyright 2019, Wiley-VCH GmbH.

human adipose-derived stem cells during 21 days. The conductivity reached ≈2.5×10^{-2} S m^{-1}, which made them suitable for bone tissue engineering applications. PAni doped with PSS was used by Chen et al. as the base for a conductive hydrogel, which they suggested using in wearable electronics.[64] They added hydrogen-bonding 2-ureido-4[1*H*]-pyrimidinone (UPy) groups as linking points to the PAni:PSS network, resulting in better stretchability, fast self-healing properties, and good printability combined with a high conductivity of 13 S m^{-1} and a linear correlation of the resistance with the external strain, allowing using it as a motion sensor.

Besides these intrinsically conductive polymers, many research groups study carbon-based fillers, such as carbon black, graphite, 2-dimensional graphene, or 1-dimensional carbon nanotubes (CNTs), which offer electrical and also thermal conductivity.[65] The next chapter gives an overview of diverse methods to produce carbon-filled polymers for different 3D printing techniques.

4.3. 3D Printing Polymers with Carbon-Based Fillers

Diverse approaches are reported in the literature to introduce carbon into 3D printed materials. As relatively large components, carbon fibers can be added to 3D printable polymers, resins, or inks to increase their conductivity and often also to improve their mechanical properties. For the possible application in wearable biomonitoring devices, Davoodi et al. suggested material jetting of highly viscous conductive inks, prepared from silicone rubber, a crosslinking agent, and milled carbon fibers with average lengths ≈140 µm.[66] The fabrication process and potential sensor geometries are depicted in **Figure 4**.[66] It should be mentioned that opposite to extrusion-based systems, the drop-on-demand printer used here works by high-speed deposition of fine droplets from highly viscous ink on the printing plate or the previous layer, respectively. Besides, the high viscosity results in lower UV curing times being necessary since the material will not much change its shape before curing, so that curing after several layers may be sufficient in many cases. For these samples, the authors found bending or tension-dependent resistances for different sensor types, respectively, and showed that these sensors could be used to detect bending motions of a finger or the elbow joint. The overall resistivity decreased significantly for milled carbon fiber contents >20%–30%, while the exact resistivity values for such conductive samples are not extractable from the paper.

Katseli et al. used a commercial FDM printing filament from ProtoPasta, containing poly(lactic acid) (PLA) and carbon black, for the production of 3D printed devices for electrochemical sensing.[67] This filament has a resistance of 2–3 × 10^4 Ω m^{-1} for 1.75 mm diameter filaments and a resistivity ≈30 Ωm in 3D printed parts parallel to the layers and ≈1.15 Ωm perpendicular to the layers[68] and can thus be used for electromagnetic shielding or similar high-ohmic applications, but is less suitable for 3D printed electronic circuits.[69] Here, the authors used anodic stripping voltammetry to detect mercury or differential pulse voltammetry to detect caffeine, respectively, and in addition, showed the potential use of the printed sensors as glucose biosensors.[67] FDM printing of ABS filled with carbon black was reported by Dawoud et al. who used commercial filament from Grand Kevan Industrial Co. Ltd and investigated the effect of different printing parameters on the strain sensing properties of sensors printed from this material.[70]

Carbon black was also used in the preparation of strain and gas-sensing 3D-printed foams by direct ink writing.[71] Wei et al. used thixotropic inks, gained by adding nanoclay, and managed to get a porous polymer/carbon black structure by sequentially removing solvent and nanoclay. They showed the possibility to detect human motion by such strain sensors as well as swelling of the foam upon exposure to volatile organic compounds, leading to increased resistance.

Graphite nanosheets were embedded in PLA to prepare FDM-printed electromagnetic interference (EMI) shielding devices, forming composites with $Ti_3C_2T_x$ nanosheets by layer-by-layer stacking hot pressing.[72] The conductivity of these layered composites was in a range of ≈1 S m^{-1} for measurements perpendicular to the layer structure and up to 300 S m^{-1} for in-plane measurements. The latter, however, was based on the highly conductive $Ti_3C_2T_x$ layers and thus cannot be taken into account for the evaluation of the conductivity of 3D printed materials.

Graphene, as a two-dimensional material, is under examination in diverse research areas in recent years, and so it is in the area of 3D printing conductive polymer composites. Jing et al. used solid-state shear milling to exfoliate and disperse graphene nanoplatelets which were embedded in linear low-density polyethylene (LLDPE) to form an FDM printable filament by a single-screw extruder.[73] The authors report that alignment of the nanoplatelets was achieved by optimizing the FDM printing speed, resulting in long-range aligned bridge-connected graphene nanoplatelet network structures. While they show thermal conductivity measurements for different samples, the electric conductivity is only mentioned to be high for graphene, but

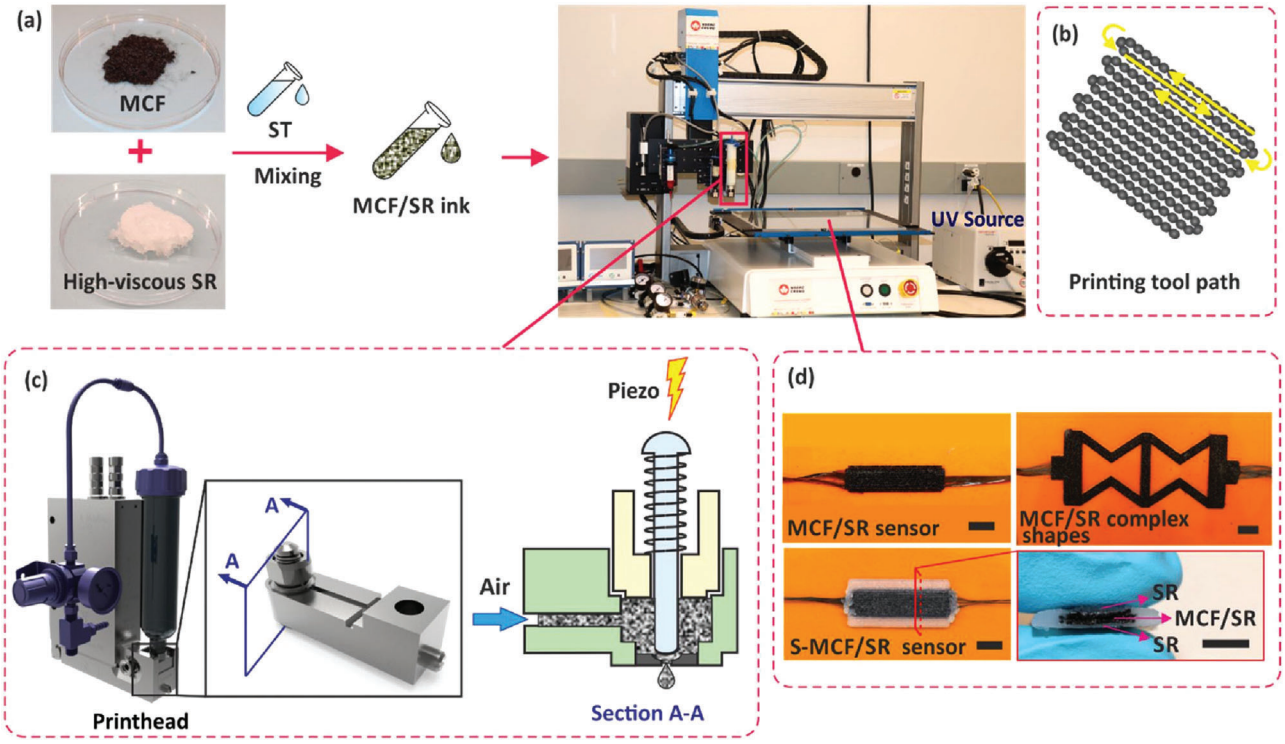

Figure 4. a) Fabrication process of milled carbon fiber/silicone rubber (MCF/SR) composites with silicone thinner (ST); b) printing tool path; c) piezoelectric-pneumatic material jetting printing head enables drop-on-demand jetting the droplets of high viscous ink (cross-section view of the printing head); d) optical images of the printed MCF/SR and sandwiched sensors (S-MCF/SR). Scale bars: 7 mm. Reproduced with permission.[66] Copyright 2020, Elsevier.

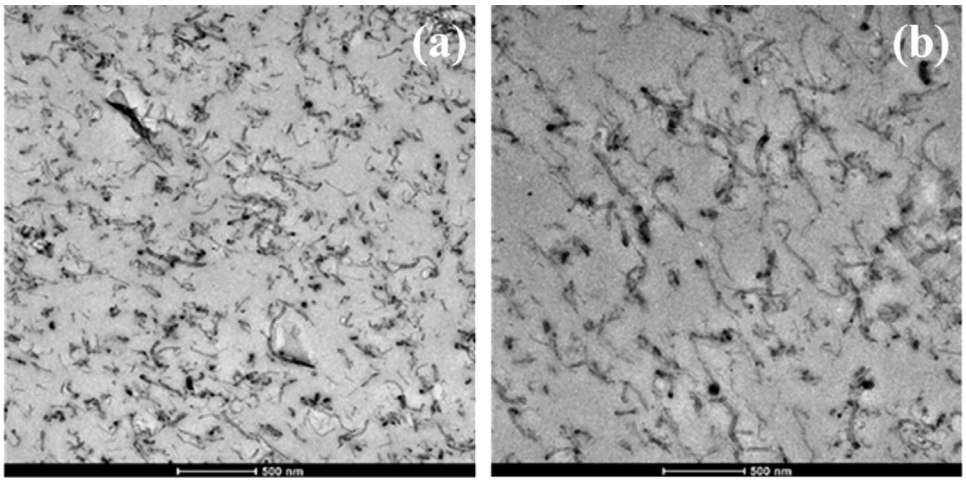

Figure 5. Transmission Electron Microscopy (TEM) images of the bi-filler composites containing **a**) polylactic acid (PLA)/1.5 wt.% GNP/4.5 wt.% MWCNT and **b**) PLA/3 wt.% GNP/3 wt.% MWCNT, respectively. Reproduced with permission under the terms of the CC-BY license.[76] Copyright 2019, the authors. Published by MDPI.

not measured. This is different from the study of de Leon et al. who used graphene/polyamide powder for selective laser sintering of a fully 3D printed electrostatic motor, working without metals,[74] and the work of Wu et al. who added electrochemically exfoliated graphene to poly(borosiloxane) (PBS) to prepare a conductive composite ink which they could use for 3D printing a gas sensor.[75]

In many cases, graphene is combined with CNTs, resulting in bi-filler composites, as depicted in **Figure 5**.[76] Ivanov et al. added industrial-grade graphene nanoplatelets and industrial-grade OH-functionalized multiwalled carbon nanotubes to PLA by melt extrusion for this purpose, comparing mono-filler and bi-filler composites. They found electrical conductivities of up to 0.06 S m^{-1} for overall filler concentrations of 6%, with similar

values for most filler ratios,[76] and values up to 6 S m^{-1} for filler concentrations of 12%.[77]

Xiang et al. filled thermoplastic polyurethane (TPU) with CNTs and graphene nanoplatelets to prepare FDM filaments from which they printed strain sensors.[78] They found conductivities of up to 1.0 S m^{-1} for the bi-filler material and slightly lower values for TPU filled with one of the components. The strain-sensing properties under cyclic stretching and releasing were found to be very good for a broad frequency range.

Adding multiwalled CNTs and graphene to poly(butylene terephthalate) (PBT), Gnanasekaran et al. prepared FDM printable filaments.[79] While no agglomerations were found, the thermally expanded graphite platelets evaporated moisture, leading to voids along the printed surface. On the other hand, high conductivities of up to 20 S m^{-1} and 2 S m^{-1} were found even for relatively small fractions of CNTs or graphene, respectively. The authors also discussed the nozzle wear upon printing PBT/CNT composite filament and showed the negative influence of printing with such an abraded nozzle.

Besides these carbon blends, many research groups use pure CNTs to make 3D printable filaments, resins, or inks conductive. Mora et al. found conductivities $\approx 10^{-1}$–1 S m^{-1} for FDM printed CNT/PLA and CNT/high-density poly(ethylene) composites with CNT contents of less than 1.5%.[80] Also blending PLA with CNTs, Shi et al. reported conductivities of 3×10^{-1} S/m reached with a local enrichment strategy.[81] Hohimer et al. added CNTs into poly(urethane) filaments and reported frequency-dependent conductivities $\approx 10^{-4}$–10^{+1} S m^{-1}, depending on layer height and CNT content of 2%–4% as well as on the measurement direction.[82] Thermoplastic polyimide (TPI) was blended with CNTs to prepare FDM filaments from which samples with resistivities ≈3 Ωm for 9 wt.% CNTs were printed, which showed a large variation upon cyclic bending.[83] Thermoplastic poly(urethane) (TPU) blended with CNTs was also used to prepare strain sensors by FDM printing, reaching very high gauge factors (sensitivities) up to 10^5.[84] By blending ABS with CNTs, Sezer, and Eren produced FDM filaments from which they printed composites with electrical conductivities up to 1 S m^{-1} for 10 wt.% CNTs.[85] Besides FDM filaments, there are also studies investigating adding CNTs to SLS powders[86] or DIW inks,[87] resulting in conductivities up to 1 S m^{-1}[86] or 10^2 S m^{-1},[87] respectively.

While carbon-based conductive polymer composites are investigated by many research groups, only few experiments are reported regarding metal-filled 3D printed composites, as shown in the next section.

4.4. 3D Printing Polymers with Metal-Based Fillers

Similar to carbon-based fillers, metal fillers can also have different shapes, typically nanowires, flakes, or particles. Nanowires with Cu core and Ag shell were synthesized by Cruz et al. and integrated into an FDM filament, resulting in a filament resistivity of only 2×10^{-5} Ωm, i.e., 4 orders of magnitude lower than the volume resistivities of the aforementioned Proto Pasta filament.[88] Using this filament, they 3D printed a conductive coil for wireless power transfer applications.

Another highly conductive FDM filament was prepared by Tan and Low who added nickel particles and $Sn_{95}Ag_4Cu_1$ to thermoplastic composite filaments from nylon-6 or high-density polyethylene (HDPE) by single-screw extrusion.[89] Electric conductivity values reached up to 2.3×10^4 S m^{-1} or 31×10^4 S m^{-1} in HDPE or nylon-6, respectively. The authors mentioned the high metal loading of 30%–35%, which they attributed to reduced melt viscosity due to the addition of the tin alloy, as compared to pure nickel particles.

Besides such purely metal-based fillers, some groups also examined metal/carbon fillers in different shapes. Wajahat et al. decorated graphene sheets with magnetite nanoparticles and added them to hydroxypropyl cellulose to prepare a conductive nanocomposite ink for extrusion-based 3D printing.[90] With this conductive ink, objects with a conductivity ≈580 S m^{-1} were produced. Due to the additional magnetic properties of this material, the authors suggested using it for 3D printing of magnet-guided cars, magnetic switches, or EMI shielding. Combining silver nanoparticles and CNTs, Xiang et al. prepared FDM printed strain sensors with a high sensitivity of 43 260 at 250% strain, with resistivities in the relaxed state $\approx 10^4$–10^6 Ωm,[91] while Wei et al. used solvent-cast 3D printing of Ag-coated carbon nanofibers in a PLA matrix to prepare smart grippers from this material with a conductivity ≈210 kS m^{-1}.[92]

5. Applications of 3D Printed Conductive Polymer Composites

Many potential applications of 3D-printed conductive polymer composites were already mentioned in Section 4. For a broader overview, several reviews exist, concentrating on specific aspects, which are exemplarily reported in this section. It should be mentioned that these reviews are not specifically directed to 3D printing, but include diverse production processes; however, the mentioned applications are in principle as well possible with 3D printed conductive polymer composites.

One of the typical applications of conductive 3D printed composites is the production of sensors, especially strain and pressure sensors, but also gas sensors. A recent overview of strain sensors produced by conductive hydrogels, partly 3D printed, is given by Tang et al.[93] Kanoun et al. concentrate on polymer/CNT nanocomposites for strain and pressure sensors, parts of which are 3D printed.[94] Tran et al. discuss intrinsically conductive polymers and their potential application in flexible sensors,[95] while Chen et al. discuss conductive polymer composites also with respect to their potential application as temperature, liquid, or vapor sensors.[96]

Another broad area of potential applications for 3D-printed conductive composites can be found in the biomedical and biotechnological area. 3D-printed conductive scaffolds based on intrinsically conductive polymers were reviewed by Alegret et al.[97] 3D printed conductive hydrogel scaffolds were described by Athukorala et al., including conductive polymers as well as conductive fillers,[98] while Distler and Boccaccini also included biosensors from conductive hydrogels.[99] 3D printing of nerve conduits for neural tissue engineering was the main aim of Yu et al., including bioprinting of cells, giving several examples of conductive printing materials.[100]

Besides these main research areas, several other applications are based on 3D printed conductive polymer composites, such as actuators,[101] EMI shielding,[102] or electrochemical energy storage,[103] besides the specific applications mentioned in the previous section.

As explained above, the main advantages of 3D printing in comparison with other polymer manufacturing techniques are the large degree of freedom, regarding the shape of printed objects as well as material combinations within one object, and the possibility to print one object at a time, which made these techniques highly feasible for rapid prototyping since their inventions. The second point, however, is also very important in research. Testing new structures, either for tissue engineering or for actuators, generally means building a specific structure once for a very first test and a few times for a statistically reliable test series. Such small series cannot be produced by injection molding due to the high costs of the mold, and subtractive production methods often do not lead to sufficient results when fine structures have to be made in a reproducible, well-defined way. 3D printing of conductive polymer-based objects is thus the optimum way to produce specimens for many research areas, as the examples in Sections 4 and 5 show.

On the other hand, the freedom of shapes and material combinations is highly important not only in research, but also for production of larger lot sizes. 3D printed sensors and actuators with a monolithic design, combining different materials with different functions to prepare an electronic part in one print, becomes more and more interesting and can also be used for mass production.[2] Additive manufacturing of partly conductive 3D substrates for tissue engineering adds a third dimension to the nowadays often electrospun two-dimensional nanofibrous substrates and enables stimulation of cell attachment, proliferation, and migration along defined paths.[104]

6. Conclusion

This review gives an overview about potential methods to prepare 3D printable conductive polymer composites, based on different material compositions, including intrinsically polymers and carbon-based as well as metal fillers, and using diverse 3D printing techniques, resulting in hydrogels, flexible or rigid objects. A broad range of conductivities is reached by these materials and techniques, resulting in an broad range of possible applications, from sensors to actuators, from biotechnology and biomedicine to EMI shielding.

Nevertheless, many challenges remain for the different additive manufacturing techniques and the chosen materials. Generally, a balance between mechanical properties (higher for larger amounts of polymer) and conductivity (higher for more conductive material) must be found for all composite materials, while 3D printing intrinsically conductive polymers needs modification of their viscosity to make them printable with an available technique and in some cases addition of binders etc., resulting in a similar balance between mechanical and electrical properties. Especially the FDM printing process has the additional problem of a high anisotropy due to the chosen printing directions and the air voids building between the strands in the final object for most materials. Further research is thus not only necessary regarding the optimization of fillers and preparation of intrinsically conductive polymers, but also with respect to the optimization of FDM and other printing techniques.

While this review cannot be comprehensive due to the large amount of papers, published during the last years, it will support the reader by offering basic knowledge about 3D printing, conductivity units and measurement techniques, and a large variety of recent approaches in this growing field of research.

Acknowledgements

This research was partly funded by the German Federal Ministry for Economic Affairs and Energy (grant no. KK5129710KT1).

Conflict of Interest

The authors declare no conflict of interest.

Keywords

3D printing, carbon black, carbon nanotubes, fused deposition modeling (FDM), graphene, graphite, metal nanoparticles, stereolithography (SLA)

Received: December 15, 2022
Revised: February 7, 2023
Published online:

[1] T. Blachowicz, G. Ehrmann, A. Ehrmann, *e-Polymers* **2021**, *21*, 549.
[2] T. Blachowicz, A. Ehrmann, *Micromachines* **2020**, *11*, 434.
[3] G. Ehrmann, T. Blachowicz, A. Ehrmann, *Polymers* **2022**, *14*, 3895.
[4] H. Yuk, B. Lu, S. Lin, K. Qu, J. Xu, J. Luo, X. Zhao, *Nat. Commun.* **2020**, *11*, 1604.
[5] Z. Římská, V. Kruesálek, J. Spacek, *Polym. Compos.* **2002**, *23*, 95.
[6] K. Kalaitzidou, H. Fukushima, L. Drzal, *Materials* **2010**, *3*, 1089.
[7] Z. Wang, L. Zhang, Y. Bayram, J. L. Volakis, *IEEE Trans. Antennas and Propag.* **2012**, *60*, 4141.
[8] M. T. Sebastian, H. Jantunen, *Appl. Ceramic Technol.* **2010**, *7*, 415.
[9] K. Gnanasekaran, T. Heijmans, S. Van Bennekom, H. Woldhuis, S. Wijnia, G. De With, H. Friedrich, *Appl. Mater. Today* **2017**, *9*, 21.
[10] T. Vilhunen, J. P. Kaipio, P. J. Vauhkonen, T. Savolainen, M. Vauhkonen, *Meas. Sci. Technol.* **2002**, *13*, 1848.
[11] M. Y. Jaffrin, H. Morel, *Med. Eng. Phys.* **2008**, *30*, 1257.
[12] D. D. Stupin, E. A. Kuzina, A. A. Abelit, A. K. Emelyanov, D. M. Nikolaev, M. N. Ryazantsev, S. V. Koniakhin, M. V. Dubina, *ACS Biomater. Sci. Eng.* **2021**, *7*, 1962.
[13] M. B. Heaney, *Electrical Conductivity and Resistivity, Electrical Measurement, Signal Processing, and Displays* (Ed. J. G. Webster), CRC Press, Boca Raton **2003**, pp. 1–14.
[14] L. Valdes, *Proc. IRE* **1954**, *42*, 420.
[15] L. J. van der Pauw, *Philips Res. Rep.* **1958**, *13*, 1.
[16] A. Ehrmann, T. Blachowicz, *Examination of Textiles with Mathematical and Physical Methods*, Springer International Publishing AG, Switzerland **2017**.
[17] J. Krupka, *Meas. Sci. Technol.* **2013**, *24*, 062001.
[18] L. Stiny, *Aktive Elektronische Bauelemente*, 3. Auflage, Springer Vieweg, Wiesbaden **2016**.
[19] P. Shah, R. Racasan, P. Bills, *Case Stud. Nondestr. Test. Eval.* **2016**, *6*, 69.
[20] E. Yankov, M. P. Nikolova, MATEC Web of Conf. **2017**, *137*, 02014.
[21] M. Sljivic, A. Pavlovic, J. Ilic, M. Stanojevic, S. Todorovic, *FME Trans.* **2017**, *45*, 348.

[22] Z. Liu, Y. Wang, B. Wu, C. Cui, Y. Guo, C. Yan, *Ind. J. Adv. Manuf. Technol.* **2019**, *102*, 2877.
[23] A. Milanovic, M. Milosevic, G. Mladenovic, B. Likozar, K. Colic, N. Mitrovic, in *Experimental and Numerical Investigations in Materials Science and Engineering* (Eds: N. Mitrovic, M. Milosevic, G. Mladenovic), Lecture Notes in Networks and Systems, Vol. *54*. CNNTech, Springer, Cham **2018**.
[24] M. Hikmat, S. Rostam, Y. M. Ahmed, *Results Eng.* **2021**, *11*, 100264.
[25] M. S. Saharudin, J. Hajnys, T. Kozior, D. Gogolewski, P. Zmarzły, *Polymers* **2021**, *13*, 1671.
[26] H. Quan, T. Zhang, H. Xu, S. Luo, J. Nie, X. Zhu, *Bioact. Mater.* **2020**, *5*, 110.
[27] M.-A. Boca, A. Sover, L. Slătineanu, *Macromol. Symp.* **2021**, *396*, 2000287.
[28] N. Badanova, A. Perveen, D. Talamona, *J. Manuf. Mater. Process.* **2022**, *6*, 109.
[29] A. Unkovskiy, P. H.-B. Bui, C. Schille, J. Geis-Gerstorfer, F. Huettig, S. Spintzyk, *Dental Mater.* **2018**, *34*, e324.
[30] J. L. Storck, G. Ehrmann, U. Güth, J. Uthoff, S. V. Homburg, T. Blachowicz, A. Ehrmann, *Polymers* **2022**, *14*, 2826.
[31] P. Ellakany, S. M. Fouda, A. A. Mahrous, M. A. Alghamdi, N. M. Aly, *Polymers* **2022**, *14*, 4103.
[32] Y.-H. Chueh, X. Zhang, J. C.-R. Ke, Q. Li, C. Wei, L. Li, *Addit. Manuf.* **2020**, *36*, 101465.
[33] C. A. Chatham, T. E. Long, C. B. Williams, *Prog. Polym. Sci.* **2019**, *93*, 68.
[34] Y. Wang, Z. Xu, D. Wu, J. Bai, *Materials* **2020**, *13*, 2406.
[35] A. Lindberg, J. Alfthan, H. Pettersson, G. Flodberg, L. Yang, *Addit. Manuf.* **2018**, *24*, 577.
[36] C. A. Chatham, T. E. Long, C. B. Williams, *Prog. Polym. Sci.* **2019**, *93*, 68.
[37] B. Sagbas, B. E. Gümüş, Y. Kahraman, D. P. Dowling, *J. Manufact. Proc.* **2021**, *70*, 290.
[38] L. A. Chavez, P. Ibave, Md. S. Hassan, S. E. Hall-Sanchez, K. Md. M. Billah, A. Leyva, C. Marquez, D. Espalin, S. Torres, T. Robison, Y. Lin, *J. Appl. Polym. Sci.* **2022**, *139*, 52290.
[39] B. Nematollahi, M. Xia, J. Sanjayan, *Front. Mater.* **2019**, *6*, 160.
[40] X. Wan, L. Luo, Y. Liu, J. Leng, *Adv. Sci.* **2020**, *7*, 2001000.
[41] L. Li, Q. Lin, M. Tang, A. J. E. Duncan, C. Ke, *Chem. – Eur. J.* **2019**, *25*, 10768.
[42] F. Puza, K. Lienkamp, *Adv. Funct. Mater.* **2022**, *32*, 2205345.
[43] S. Naghieh, Md. Sarker, N. K. Sharma, Z. Barhoumi, X. Chen, *Appl. Sci.* **2020**, *10*, 292.
[44] Y. Wang, Y. Ding, X. Guo, G. Yu, *Nano Res.* **2019**, *12*, 1978.
[45] Q. Peng, J. Chen, T. Wang, X. Peng, J. Liu, X. Wang, J. Wang, H. Zeng, *InfoMat* **2020**, *2*, 843.
[46] J. L. Storck, M. Dotter, B. Brockhagen, T. Grothe, *Crystals* **2020**, *10*, 1158.
[47] M. Dotter, J. L. Storck, M. Surjawidjaja, S. Adabra, T. Grothe, *Appl. Sci.* **2021**, *11*, 5834.
[48] B. Guo, Z. Ma, L. Pan, Y. Shi, *J. Polym. Sci. B Polym. Phys.* **2019**, *57*, 1606.
[49] L. Li, Y. Shi, L. Pan, Y. Shi, G. Yu, *J. Mater. Chem. B* **2015**, *3*, 2920.
[50] Y. Shi, C. Ma, L. Peng, G. Yu, *Adv. Funct. Mater.* **2015**, *25*, 1219.
[51] S. Ma, F. Ribeiro, K. Powell, J. Lutian, C. Møller, T. Large, J. Holbery, *ACS Appl. Mater. Interfaces* **2015**, *7*, 21628.
[52] H. Yuk, B. Lu, S. Lin, K. Qu, J. Xu, J. Luo, X. Zhao, *Nat. Commun.* **2020**, *11*, 1604.
[53] H. Rastin, B. Zhang, J. Bi, K. Hassan, T. T. Tung, D. Losic, *J. Mater. Chem. B* **2020**, *8*, 5862.
[54] D. N. Heo, S.-J. Lee, R. Timsina, X. Qiu, N. J. Castro, L. G. Zhang, *Mater. Sci. Eng., C* **2019**, *99*, 582.
[55] N. J. Castro, J. O'brien, L. G. Zhang, *Nanoscale* **2015**, *7*, 14010.
[56] H. Wei, M. Lei, P. Zhang, J. Leng, Z. Zheng, Y. Yu, *Nat. Commun.* **2021**, *12*, 2082.
[57] G. Scordo, V. Bertana, L. Scaltrito, S. Ferrero, M. Cocuzza, S. L. Marasso, S. Romano, R. Sesana, F. Catania, C. F. Pirri, *Mater. Today Commun.* **2019**, *19*, 12.
[58] P. Zhang, N. Aydemir, M. Alkaisi, D. E. Williams, J. Travas-Sejdic, *ACS Appl. Mater. Interfaces* **2018**, *10*, 11888.
[59] E. Tomaskovic-Crook, P. Zhang, A. Ahtiainen, H. Kaisvuo, C.-Y. Lee, S. Beirne, Z. Aqrawe, D. Svirskis, J. Hyttinen, G. G. Wallace, J. Travas-Sejdic, J. M. Crook, *Adv. Healthcare Mater.* **2019**, *8*, 1900425.
[60] A. T. Cullen, A. D. Price, *Synth. Met.* **2018**, *235*, 34.
[61] S. Vijayavenkataraman, S. Kannan, T. Cao, J. Y. H. Fuh, G. Sriram, W. F. Lu, *Front. Bioeng. Biotechnol.* **2019**, *7*, 266.
[62] S. Vijayavenkataraman, S. Zhang, S. Thaharah, G. Sriram, W. F. Lu, J. Y. H. Fuh, *Polymers* **2018**, *10*, 753.
[63] A. Wibowo, C. Vyas, G. Cooper, F. Qulub, R. Suratman, A. I. Mahyuddin, T. Dirgantara, P. Bartolo, *Materials* **2020**, *13*, 512.
[64] J. Chen, Q. Peng, T. Thundat, H. Zeng, *Chem. Mater.* **2019**, *31*, 4553.
[65] H.-Y. Zhao, M. -Y. Yu, J. Liu, X. Li, P. Min, Z. -Z. Yu, *Nano-Micro Lett.* **2022**, *14*, 129.
[66] E. Davoodi, H. Fayazfar, F. Liravi, E. Jabari, E. Toyserkani, *Addit. Manuf.* **2020**, *32*, 101016.
[67] V. Katseli, A. Economou, C. Kokkinos, *Electrochem. Commun.* **2019**, *103*, 100.
[68] Protopasta, Conductive PLA, https://www.proto-pasta.com/pages/conductive-pla (accessed: December 2022).
[69] N. Grimmelsmann, Y. Martens, P. Schäl, H. Meissner, A. Ehrmann, *Procedia Technol.* **2016**, *26*, 66.
[70] M. Dawoud, I. Taha, S. J. Ebeid, *J. Manuf. Proc.* **2018**, *35*, 337.
[71] P. Wei, H. Leng, Q. Chen, R. C. Advincula, E. B. Pentzer, *ACS Appl. Polym. Mater.* **2019**, *1*, 885.
[72] T.-B. Ma, H. Ma, K.-P. Ruan, X.-T. Shi, H. Qiu, S.-Y. Gao, J.-W. Gu, *Chin. J. Polym. Sci.* **2022**, *40*, 248.
[73] J. Jing, Y. Chen, S. Shi, L. Yang, P. Lambin, *Chem. Eng. J.* **2020**, *402*, 126218.
[74] A. C. De Leon, B. J. Rodier, C. Bajamundi, A. Espera, P. Wei, J. G. Kwon, J. Williams, F. Ilijasic, R. C. Advincula, E. Pentzer, *ACS Appl. Energy Mater.* **2018**, *1*, 1726.
[75] T. Wu, E. Gray, B. Chen, *J. Mater. Chem. C* **2018**, *6*, 6200.
[76] E. Ivanov, R. Kotsilkova, H. Xia, Y. Chen, R. Donato, K. Donato, A. Godoy, R. Di Maio, C. Silvestre, S. Cimmino, V. Angelov, *Appl. Sci.* **2019**, *9*, 1209.
[77] G. Spinelli, P. Lamberti, V. Tucci, R. Ivanova, S. Tabakova, E. Ivanov, R. Kotsilkova, S. Cimmino, R. Di Maio, C. Silvestre, *Compites, B. Eng.* **2019**, *167*, 467.
[78] D. Xiang, X. Zhang, Z. Han, Z. Zhang, Z. Zhou, E. Harkin-Jones, J. Zhang, X. Luo, P. Wang, C. Zhao, Y. Li, *J. Mater. Sci.* **2020**, *55*, 15769.
[79] K. Gnanasekaran, T. Heijmans, S. Van Bennekom, H. Woldhuis, S. Wijnia, G. De With, H. Friedrich, *Appl. Mater. Today* **2017**, *9*, 21.
[80] A. Mora, P. Verma, S. Kumar, *Compites, B. Eng.* **2020**, *183*, 107600.
[81] S. Shi, Y. Chen, J. Jing, L. Yang, *RSC Adv.* **2019**, *9*, 29980.
[82] C. J. Hohimer, G. Petrossian, A. Ameli, C. Mo, P. Pötschke, *Addit. Manuf.* **2020**, *34*, 101281.
[83] W. Ye, W. Wu, X. Hu, G. Lin, J. Guo, H. Qu, J. Zhao, *Composite Sci. Technol.* **2019**, *182*, 107671.
[84] D. Xiang, X. Zhang, Y. Li, E. Harkin-Jones, Y. Zheng, L. Wang, C. Zhao, P. Wang, *Composites, B. Eng.* **2019**, *176*, 107250.
[85] H. K. Sezer, O. Eren, *J. Manufact. Proc.* **2019**, *37*, 339.
[86] X. Gan, J. Wang, Z. Wang, Z. Zheng, M. Lavorgna, A. Ronca, G. Fei, H. Xia, *Mater. Des.* **2019**, *178*, 107874.
[87] X. Wan, F. Zhang, Y. Liu, J. Leng, *Carbon* **2019**, *155*, 77.
[88] M. A. Cruz, S. Ye, M. J. Kim, C. Reyes, F. Yang, P. F. Flowers, B. J. Wiley, *Part. Part. Syst. Charact.* **2018**, *35*, 1700385.
[89] J. C. Tan, H. Y. Low, *Addit. Manuf.* **2018**, *23*, 294.
[90] M. Wajahat, J. H. Kim, J. Ahn, S. Lee, J. Bae, J. Pyo, S. K. Seol, *Carbon* **2020**, *167*, 278.

[91] D. Xiang, X. Zhang, E. Harkin-Jones, W. Zhu, Z. Zhou, Y. Shen, Y. Li, C. Zhao, P. Wang, *Composites, A Appl. Sci. Manufact.* **2020**, *129*, 105730.
[92] H. Wei, X. Cauchy, I. O. Navas, Y. Abderrafai, K. Chizari, U. Sundararaj, Y. Liu, J. Leng, D. Therriault, *ACS Appl. Mater. Interfaces* **2019**, *11*, 24523.
[93] L. Tang, S. Wu, J. Qu, L. Gong, J. Tang, *Materials* **2020**, *13*, 3947.
[94] O. Kanoun, A. Bouhamed, R. Ramalingame, J. R. Bautista-Quijano, D. Rajendran, A. Al-Hamry, *Sensors* **2021**, *21*, 341.
[95] V. V. Tran, S. Lee, D. Lee, T.-H. Le, *Polymers* **2022**, *14*, 3730.
[96] J. Chen, Y. Zhu, J. Huang, J. Zhang, D. Pan, J. Zhou, J. E. Ryu, A. Umar, Z. Guo, *Polym. Rev.* **2021**, *61*, 157.
[97] N. Alegret, A. Dominguez-Alfaro, D. Mecerreyes, *Biomacromolecules* **2019**, *20*, 73.
[98] S. S. Athukorala, T. S. Tran, R. Balu, V. K. Truong, J. Chapman, N. K. Dutta, N. Roy Choudhury, *Polymers* **2021**, *13*, 474.
[99] T. Distler, A. R. Boccaccini, *Acta Biomater.* **2020**, *101*, 9.
[100] X. Yu, T. Zhang, Y. Li, *Polymers* **2020**, *12*, 1637.
[101] F. Hu, Y. Xue, J. Xu, B. Lu, *Front. Robot. AI* **2019**, *6*, 114.
[102] M. Wang, X.-H. Tang, J.-H. Cai, H. Wu, J.-B. Shen, S.-Y. Guo, *Carbon* **2021**, *177*, 377.
[103] V. Egorov, U. Gulzar, Y. Zhang, S. Breen, C. O'dwyer, *Adv. Mater.* **2020**, *32*, 2000556.
[104] E. Tanzli, A. Ehrmann, *Appl. Sci.* **2021**, *11*, 6929.